Baghdad Science Journal

Volume 22 | Issue 6 Article 4

6-17-2025

Green Synthesis, Characterization, Antimicrobial and Anticancer Studies of Vanadium Oxide Nanoparticles Using *Vitex Agnus Castus* Extract

Saba H. Mahdi
Department of Chemistry, College of Education for Pure Sciences (Ibn Al-Haitham), University of Baghdad, Iraq, saba.harbi2104p@ihcoedu.uobaghdad.edu.iq

Lekaa K. Abdul karem
Department of Chemistry, College of Education for Pure Sciences (Ibn Al-Haitham), University of Baghdad, Iraq, likaa.k.a@ihcoedu.uobaghdad.edu.iq

How to Cite this Article

Mahdi, Saba H. and karem, Lekaa K. Abdul (2025) "Green Synthesis, Characterization, Antimicrobial and Anticancer Studies of Vanadium Oxide Nanoparticles Using *Vitex Agnus Castus* Extract," *Baghdad Science Journal*: Vol. 22: Iss. 6, Article 4.
DOI: https://doi.org/10.21123/2411-7986.4954

BAGHDAD SCIENCE JOURNAL 2025;22(6):1774–1784

RESEARCH ARTICLE

Green Synthesis, Characterization, Antimicrobial and Anticancer Studies of Vanadium Oxide Nanoparticles Using *Vitex Agnus Castus* Extract

Saba H. Mahdi, Lekaa K. Abdul karem *

Department of Chemistry, College of Education for Pure Sciences (Ibn Al-Haitham), University of Baghdad, Iraq

ABSTRACT

This study, vanadium oxide nanoparticles were synthesized using the biosynthesis method. The resulting VO_2 NPs are characterized by their cost-effectiveness, ease of use, and safety. Vanadium Nano oxide was prepared from vanadium sulfate monohydrate with a plant extract of *Vitex agnus castus* at a sodium hydroxide concentration of 0.1 M. The reaction was carried out in an alkaline medium at pH range of 8–12, which were characterized by using many techniques such as; Fourier transform IR spectroscopy, ultraviolet-visible spectroscopy, x-ray diffraction XRD, transmission electron microscopy TEM, scanning electron microscopy SEM and EDX pattern. The crystal size of nanoparticles, determined using Debye Scherer's equation in X-ray diffraction, was measured at 16.66 nm, while vanadium oxide nanoparticles size was calculated by using SEM and TEM. Antimicrobial activities of vanadium oxide nanoparticles were studied against four strains of bacteria, two types of *Staphylococcus aureus, Streptococcus pneumonia*as gram positive, two types of *Proteus mirabilis, Escherichia coli* as gram negative and one type of fungal such as *Candida albicans* to test the antifungal properties. Vanadium oxide nanoparticles showed different efficacy against these antimicrobials. Furthermore, the study explored the anticancer potential of the synthesized vanadium oxide nanoparticles on the SW480 cell line for colorectal cancer using the MTT assay at different concentrations. The results indicated that an increase in concentration led to a corresponding increase in the percentage of inhibition. The calculated inhibition half of the cells (IC_{50}) was found to be 53 mg/ml, suggesting that these nanoparticles could be potentially used for the selective treatment of colon cancer.

Keywords: Antimicrobial activity, Cell line SW480, Nanoparticles, Vitex agnus castus, X-ray diffraction

Introduction

Nano science and nanotechnology encompass the study and application of minuscule entities applicable across various scientific domains such as chemistry, biology, physics, materials science, and engineering.[1–4] In recent years, vanadium Nano composites have gained significant importance due to their physical and chemical properties, finding applications in sensors,[5–8] electro chromic and optical switches,[9] as electrode material for electrochemical capacitors and in solar cell windows.[10,11] Nanoparticle properties (chemical, physical, and biological) at the Nano scale can significantly differ from those of both individual atoms and molecules and the resulting bulk material.[12] *Vitex agnus castus*, native to the Mediterranean region, is also known as *Vitex*, chaste tree, Abraham's balm, or monk's pepper. It is one of the few *Vitex* species that grow in temperate regions, typically found in tropical and subtropical flowering plants.[13] The leaves, flowers, and/or berries can be eaten directly from the plant or used to make a decoction, traditional tincture, cider-vinegar tincture, syrup, or elixir. The most effective method of taking *Vitex* is as a 1:1 fluid extract in the morning, known to interact with hormonal circadian rhythms.[14] In the field of technology and manufacturing, vanadium oxide material has gained

Received 20 September 2023; revised 1 March 2024; accepted 3 March 2024.
Available online 17 June 2025

* Corresponding author.
E-mail addresses: saba.harbi2104p@ihcoedu.uobaghdad.edu.iq (S. H. Mahdi), likaa.k.a@ihcoedu.uobaghdad.edu.iq (L. K. Abdul karem).

https://doi.org/10.21123/2411-7986.4954

attention for its ease of preparation, affordability, and versatility. VO_2 also offers safety-related properties and high energy density.[15] Among the well-known group of oxides, synthetic vanadium has been widely studied for over a decade due to its electrochemical properties and high stability.[16,17] In recent research, a facial green synthesis technique was developed for preparing VO_2 utilizing *Vitex agnus castus*. The aim of this work is to prepare vanadium oxide nanoparticles through green synthesis, using a plant extract from *Vitex agnus castus*. Furthermore, the study aims to estimate the antimicrobial activity against various organisms and assess the toxicity of the synthesized 4 nanoparticles.

Materials and methods

The herb was taken from local sources, collected, and distinguished. Sodium hydroxide NaOH from India's Alpha Chemica and hydrate vanadium sulfate $VOSO_4.H_2O$ from England were utilized. To characterize and identify all the compounds, a verity of spectroscopic and microscopic methods was employed, including a PLC Centrifuge, a Faithful model WHL. 25ABElectric Oven, a RADWAG model AS 220C1Sensitive Electronic Balance, a FINETEDISCL Shaking Water Bath, pH tapes, UV-Vis. measure (Shimadzu 160/UV), FTIR kind spectroscopy (8500s), X-Ray (XRD) diffraction (PW1730Phillips/Holland), MIRAIIIFESEM model from Czech, TEM with the model number EM10C-100 Kv. The intensity of the resulting color after adding MTT dye was measured using a micro plate reader (DNM-9602G).

Preparation of plant extract

After being rinsed with tap water to eliminate any clinging contaminants, fresh herbs are thoroughly dried after being removed from the water, and then left to dry in air for overnight. Following this, the herbs are ground to simplify the extraction process. After adding 20 grams of the herbs to 200 milliliters of deionized water and continuously stirring with a magnetic stirrer for thirty minutes at a temperature ranging between sixty and seventy degrees Celsius, the mixture is allowed to cool at room temperature before being used. The filtering process takes place in the centrifuge. The plant extract is collected and stored in test tubes, rotated at a speed of 4000 revolutions per minute in the centrifuge to remove any remaining debris and fibres while maintaining the integrity of the filter.[18]

Preparation of vanadium nanoparticles VO_2 NPs

The vanadium oxide nanoparticles were prepared using an environmentally friendly synthesis method. After stirring for half an hour, 100 millilitres of filtered plant extract solution were added to 100 millilitres of aqueous vanadium sulfate solution with a concentration of 1.81 grams per 100 millilitres (18.1 g/ml). Subsequently, 50 millilitres of sodium hydroxide solution, containing 2 grams, was added drop wise until the pH value reached 12. After one hour at a temperature of seventy degrees, a change in hue and the formation of precipitate were observed. After being left overnight, the mixture was separated using a centrifuge. The resulting samples were rinsed multiple times with deionized water and then subjected to drying in an electric oven set to 300 degrees Celsius for three hours.[19]

Biological activity

The well diffusion method was used to investigate the efficiency of the herb and vanadium nanoparticles against pathogenic bacteria under aerobic circumstances. The inhibitory activity against all pathogenic microorganisms was tested using Mueller-Hinton agar. After growing each indicator microorganism in a nutrient broth (two gram-negative bacteria*: E. coli, P. mirabilis,* and two gram-positive bacteria*: Staph. aureus, S.pneumoniae, and C. albicans,* as fungus), agar plates were inoculated with ($1.5*10^8$ (CFU)/ml for bacteria and $1.5*10^6$ (CFU)/ml for mold respectively, in comparison to 0.5 McFarland tube. In Mueller-Hinton agar plate, wells (6 mm) were cut and 100 μl of nanoparticles were added to each well. For bacteria, plates were incubated at 37˚C for 24 hrs. However, for the fungi species plates were incubated at 28˚C for 72 hrs. The diameter of inhibitory zones (mm) was used to assess activity.[20] The samples were evaluated at the University of Baghdad's Environmental Laboratory Center.

Cytotoxic assays

The MTT assay was employed to determine the effectiveness of vanadium nanoparticles on the colon cancer cell lineSW480 and the degree to which these nanoparticles reduce the activity of these cells by applying the calorimetric technique to evaluate the cell's metabolic activity.[21] This method involved the use of the MTT as a dye, 3-(4,5-dimethylthiazol-2-yl)-2,5-diphenyl tetrazolium bromide with a distinctive color[22] to examine the vitality of cells. The procedure was done as follow:

First day

A- The cells were poured in a 96-well micro plate.
B- Counting cells was done by using trypan blue, about 1×10^4 cells were cultured in each well. After the cells were cultivated, the 96-well plate was placed in an incubator at 37°C for 24 hours until 60% of the well surface was filled, otherwise more time is needed.

Second day

A- The cells were treated with 0.01 g/ml concentration of vanadium nanoparticles.

Different dilutions were used for the treatment of cells (7.81–500 by double dilution); all dilutions were prepared in sterile micro tubes.

After emptying the supernatant of each well by the sampler, 100 μl of each dilution was added to the wells. The pouring pattern was drawn and eight wells were considered.

Third day

A. Adding MTT dye

After 24 hours, the medium was removed and 100 μl of MTT solution (concentration 0.5 mg/ml) was added to the plates in the dark and placed in the incubator for 4 hours. Then, the top medium of the wells was removed with a sampler and 100 μl of DMSO was added to the wells, then placed on a shaker for 20 minutes (at this stage, the container should be covered so as not to be exposed to light). Finally, the intensity of the resulting color was read by a micro plate reader (DNM-9602G) at a wavelength of 570 nm.

Results and discussion

FTIR spectra

The FTIR spectra of VO_2 NPs are presented in the range (400–4000) cm^{-1}, as shown in Fig. 1 below. The spectrum of VO_2 NPs was prepared from *Vitex agnus castus*. Fig. 2 presents different types of vibration bands located at (937–424) cm^{-1} which were attributed to oxygen bonds V=O stretching mode. The values (3425, 1654, and 1415) cm^{-1}represent the vibration stretching of O-H, C=C and C=O, respectively, possibly indicating the presence of organic materials residues.[23–25]

The UV-visible spectrum

The ultraviolet-visible spectroscopy technique was employed to verify the optical characteristics of the nanoparticles synthesized using plant extract and vanadium, as depicted in the accompanying images. The ultraviolet-visible spectrum refers to a segment of the electromagnetic spectrum characterized by shorter wavelengths than visible light. Ultraviolet radiation has a broader spatial extent than X-rays. This nomenclature is derived from the fact that the wavelength associated with the violet colour, which is the shortest among the colours present in the electromagnetic spectrum, is included within the range of 10 nm to 400 nm. Furthermore, the energy levels of ultraviolet photons span from 3 to 124 electron volts (eV).[26,27] The absorption peak of the transition holes between vanadium and oxygen in the ultraviolet spectrum of vanadium oxide, produced from plant extract, was seen at 345 nm. To further support these findings, the energy gap was determined utilizing the following Eq. (1):

$$Eq = \frac{1240}{\lambda} = 1240 \ / \ 345 = 3.6 \ eV \quad (1)$$

X-ray diffraction (XRD)

X-ray diffraction patterns have historically been employed to reveal significant characteristics within a compound, including identifying crystalline phases and their respective properties. The X-ray diffraction technique allows for determining the sample's position (angle) and intensities of the diffracted X-ray beam, thereby providing valuable information about the sample.[28] Fig. 2 shows a picture of as-grown products taken with XRD spectroscopy. The diffraction pattern reveals distinct peaks with relatively small half-height breadths. The observed diffraction occurs at angles of position [2θ] (12.16, 18.67, 25.76, 29.05, 30.64, 38.00, 41.38, 58.18, and 59.46) ° corresponding to the diffractive crystal planes of Millers coefficients (200, –201, 110, –401, 400, 401, 112, 113, and –711) of VO_2 nanoparticles. These angles align with the standard diffraction peaks of VO_2 (JCPDS Card No. 65–7960).[29,30] closely corresponding to the pattern found for VO_2. Consequently, it has been conclusively proven that the products are VO_2 with a monoclinic crystalline structure, as detailed in Table 1.

Using the Debye Scherer's equation,[31] an average crystal size was determined to be 16.66 nm, and this value can be found in Table 1.

Energy dispersive X-ray (EDX)

The energy dispersive X-ray (EDX) spectrum of VO_2 NPs in Fig. 3 reveals the presence of vanadium and oxygen elements. The spectrum exhibits characteristic peaks associated with these elements, with

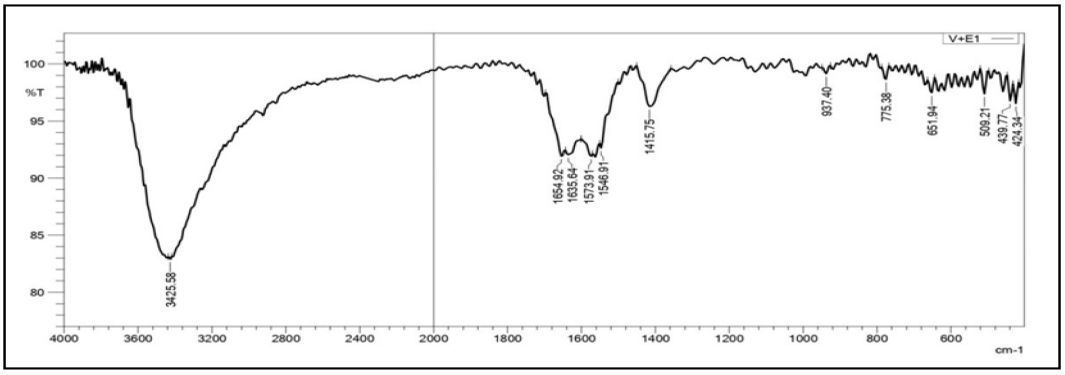

Fig. 1. FTIR spectrum of VO_2 NPs.

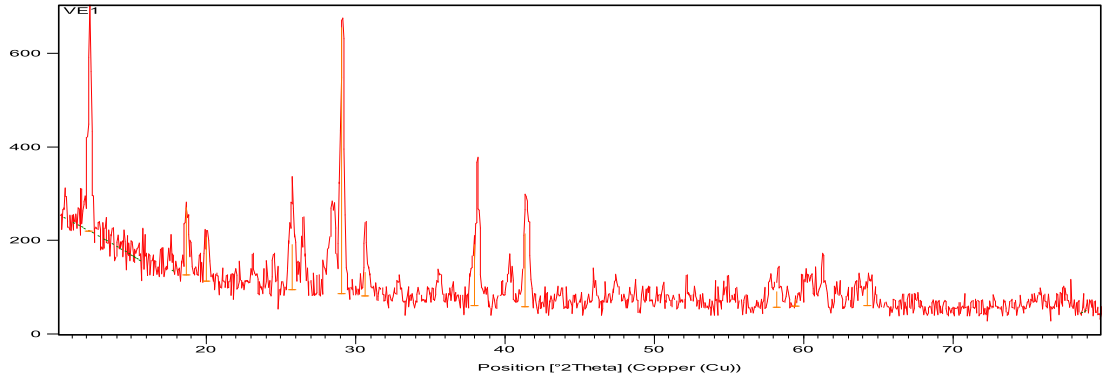

Fig. 2. XRD of VO_2 NPs.

Table 1. The data of XRD for VO_2 NPs.

Pos. [2θ]	Height [cts]	FWHM [2θ]	Dp(nm)	Dp Average(nm)
12.16	3.23	4.00	2.09	16.66
18.67	144.29	0.4604	18.28	
20.03	94.56	0.5154	16.36	
25.76	96.88	0.6856	12.42	
29.05	569.38	0.2723	31.50	
30.64	49.86	1.3960	6.17	
38.00	131.07	0.3676	23.89	
41.38	156.61	0.4660	19.02	
58.18	34.72	2.1845	4.35	
59.46	15.03	0.0013	32.55	

67.6% attributed to vanadium and 32.4% to oxygen. These findings confirm that the synthesized nanoparticles show a high level of purity. Furthermore, the estimates derived from the EDX experiment are consistent with the elemental theoretical calculations. [32]

Field emission scanning electron microscopy (FE-SEM)

It is one of the highly accuracy techniques used to characterize nanoparticles on a Nano scale level through SEM images by scanning the sample with a focused beam of activated electrons. This process gives important information about the sample, including its crystalline arrangement, his to chemical composition, and surface morphology. [33] This can be seen through the shapes of the SEM images, and the sizes of the diameters of its grains, ranging between (15.63–48.97 nm). This confirms the validity of the formation of vanadium nanoparticles within the nanoscale using the *Vitex agnus castus* extract as exposed in Fig. 4.

Transmission electron microscopy (TEM)

Based on TEM images in Fig. 5, it was determined that the morphology of VO_2 NPs was aggregated. The precision of the measurements prevents a precise estimation of the sample's shape. However, it appears to contain zero-dimensional measurements of an amorphous spherical structure within the sample, with all dimensions falling within the Nano scale, which is highly preferred in surface chemistry for nanomaterial's. [34,35]

Antimicrobial studies

By employing the well plate method in nutritional agar, the synthesized VO_2 NPs in this study were

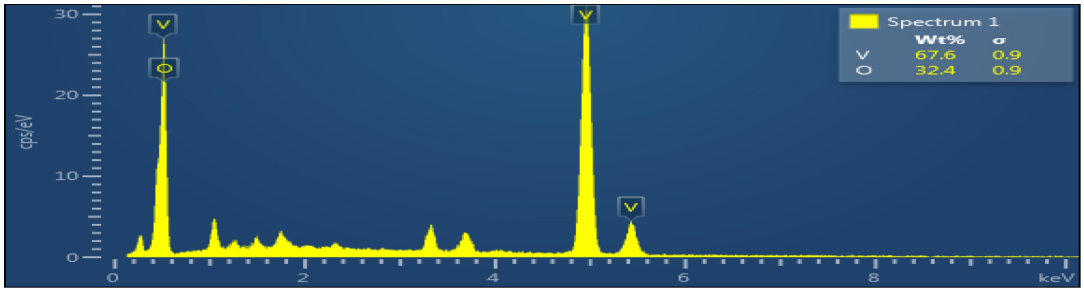

Fig. 3. The EDX of VO_2 NPs.

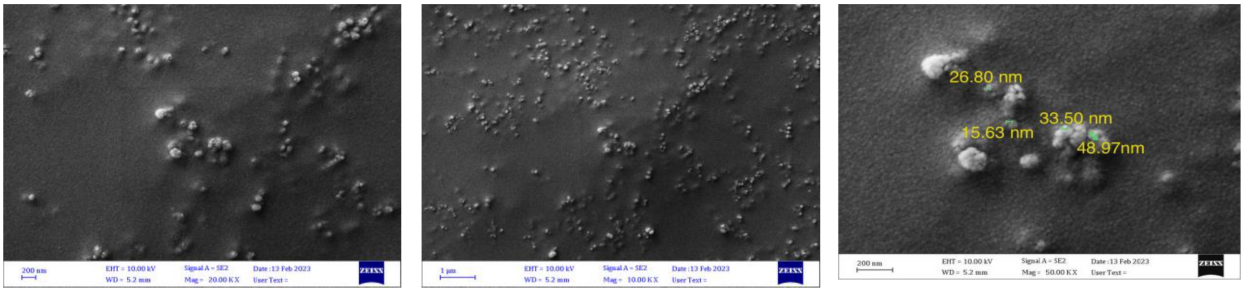

Fig. 4. SEM images of VO_2 NPs.

evaluated against four types of bacteria (G+: *Staph. aureus, S. pneumoniae),* two negative *(G-: P. mirabilis, E. coli*) and one type of fungus (*C. albicans*). The biological activity of the vanadium nanoparticles was measured in millimetres (mm) by measuring the inhibition zone diameter (ZI) around each hole with (DMSO) used as a solvent.[36–38] The dishes showed variation in the activity of the substance, revealing that vanadium nanoparticles showed the highest activity against gram positive bacteria (23 and 23.9) mm and *C. albicans* (22.9 mm), while the herb displayed the highest activity against *E. Coli* (18.9 mm). The mean of inhibition zone diameter (average); Std. Deviation (standard Deviation) and CI (Confidence limit) were calculated as shown in Table 2, Figs. 6 and 7. The precise mechanism by which Vanadium ions exert their antibacterial activity needs further study. Chelate complexes inactivate crucial cellular enzymes involved in the metabolic pathways of these microorganisms. Consequently, this enhances the lipophilic properties of the central metal atom, facilitating its more efficient penetration through the microorganism's lipid layer and resulting in a more aggressive destruction of the microorganisms. The antibacterial activity is likely a result of the electrostatic interaction between the negatively charged cell membrane of the microbe and the positively charged nanoparticles. Furthermore, the build-up of Viral Nanoparticles within the cellular cavities leads to the cell membrane becoming permeable, ultimately resulting in cell demise.[39,40]

Viability and cytotoxicity of cells utilizing assays (MTT)

This method involved the use of the SW480 cancer cell line, employing as a dye, 3-(4,5-dimethylthiazol-2-yl)-2,5-diphenyl tetrazolium bromide (MTT) as a dye to examine the vitality of cells.[41] The study results showed that vanadium oxides have a significant toxic effect on cancer cells at different concentration (7.81–500 mg/ml), as elaborated below. In this

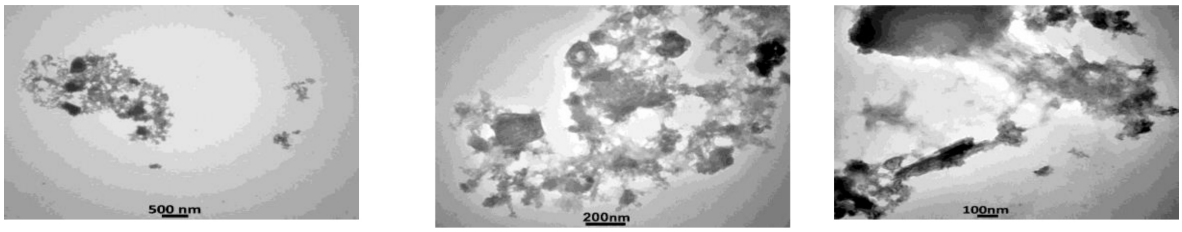

Fig. 5. TEM images of VO_2 NPs.

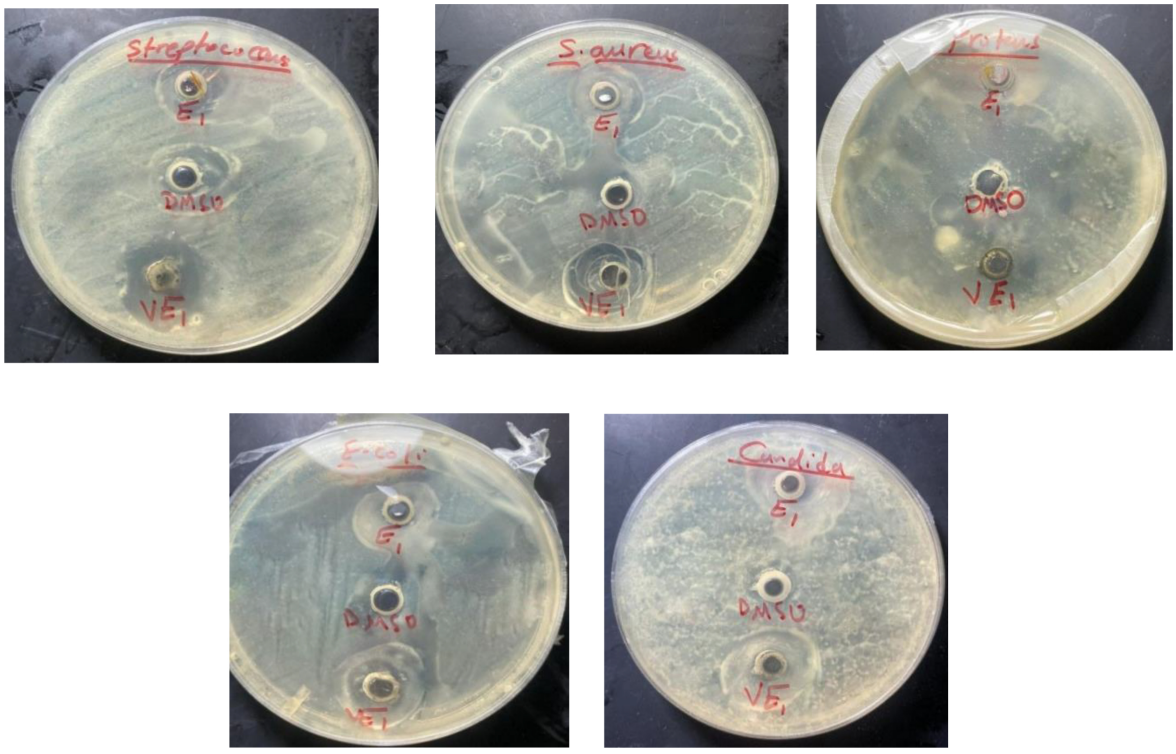

Fig. 6. Zone of growth inhibition against antimicrobial.

Table 2. Inhibition zone (mm) of VO_2 NPs from the Vitex agnus castus extract.

Compound	Organism	Mean ± Std. Deviation	95% CI of Mean
Vitex Agnus Castus	*Staph. aureus*	18.7 ± 0.20	17.5–18.5
	S.pneumoniae	19 ± 0.2	18.5–19.5
	E. coli	21.17 ± 0.15	20.79–21.55
	P. mirabilis	18.7 ± 0.6	17.19–20.21
	C. albicans	18.9 ± 0.25	18.3–19.59
VO_2 NPs	*Staph. aureus*	23.0 ±0.2	22.52–23.55
	S.pneumoniae	23.9± 0.11	23.65–24.22
	E. coli	18.9 ± 0.3	18.2–19.73
	P. mirabilis	20.1 ± 0.2	19.65–20.68
	C. albicans	22.9 ± 0.15	22.55–23.31

Where: mean (average); Std. Deviation (standard Deviation) and CI (Confidence limit).

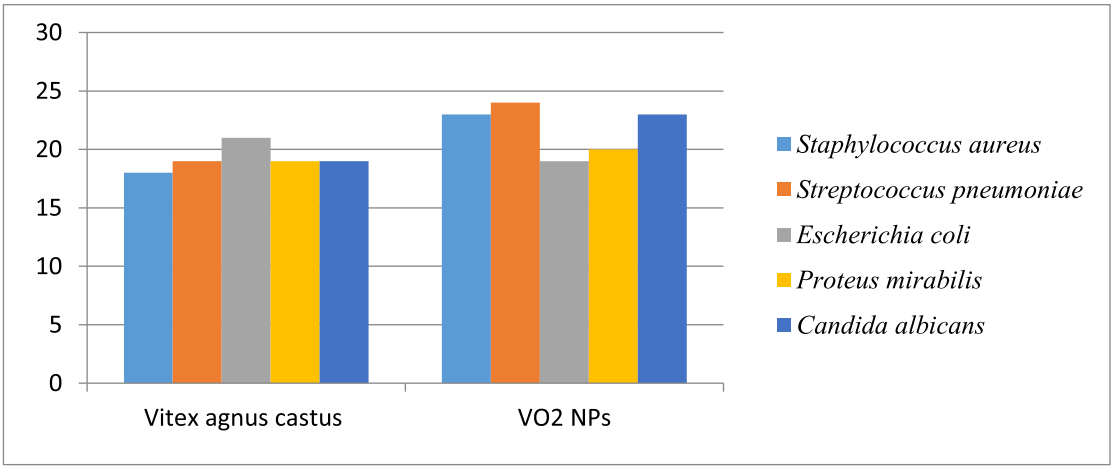

Fig. 7. The (ZI) mm of VO_2 NPs.

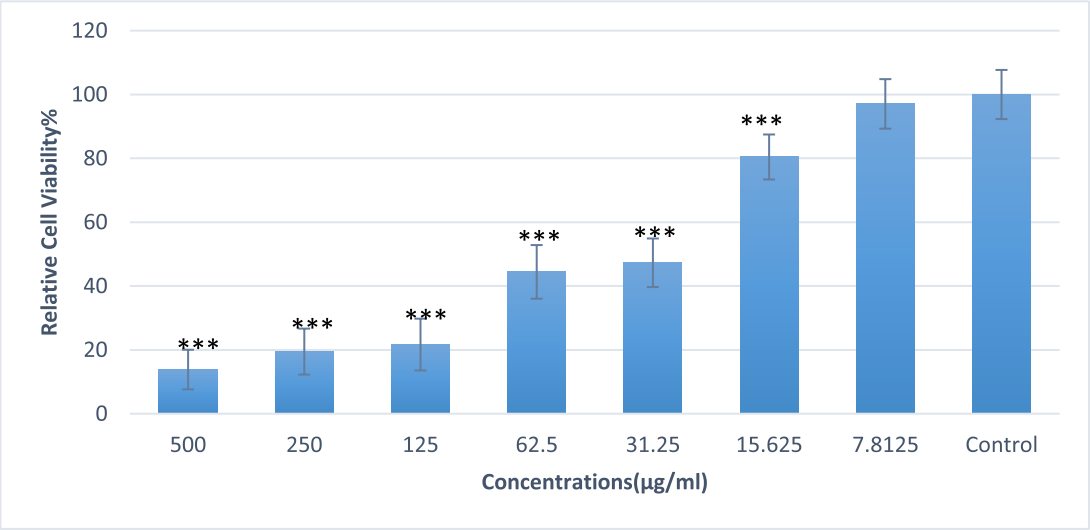

Fig. 8. The percentage of viability in the cells of the cancer line SW480 after adding VO_2 NPs.

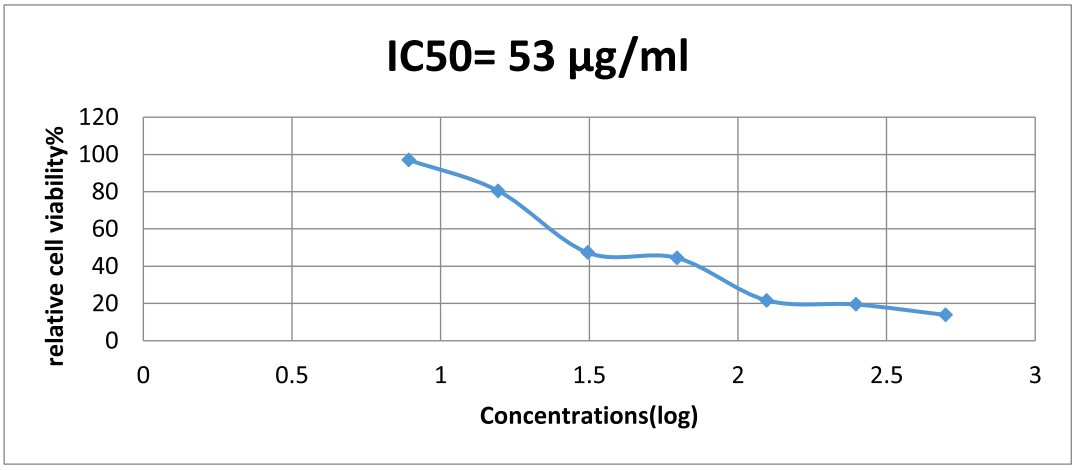

Fig. 9. The half inhibition fifty (IC_{50}) of VO_2 NPs.

study, the extent of the toxic effect was estimated by extracting the percentage of growth inhibition rate for 72 hours at a temperature of 37°C. [42,43]

The lowest cell viability percentage (13.83%) was observed, corresponding to the highest inhibition percentage for the cell line colon cancer at concentration (500 μg/mL) after treatment with the prepared nanoparticles as shown in Table 3. The results showed that the compound concentrations essential in determining the percentage of cell inhibition. It was found that the increased concentration reduces the percentage of viability, thereby increasing the inhibition percentage of cell growth in the cancerous cell line, as indicated in Table 3 and Fig. 8. The intensity of the resulting color was notably observed at a wavelength of 570 nm. Human cells are susceptible to the cytotoxic effects of nanoparticles via many mechanisms, including DNA damage, assimilation of free nanoparticles, site-specific cytotoxicity, production of reactive oxygen species (ROS), and generation of free radicals, among others. Additionally, the heightened toxicity of vanadium nanoparticles towards colon cancer cells can be attributed to their pro-oxidant properties, given that vanadium is a pro-oxidant that induces ROS production, increased lipid oxidation, and mitochondrial dysfunction in cancer cells compared to normal cells.

One of the crucial findings from the conducted tests on vanadium oxide nanoparticles with the SW480 cancer cell line is the determination of the half-inhibition concentration (IC_{50}). [44,45] This concentration signifies the point at which almost half of the cells are killed. In the case of the interaction between nanoparticles and the colon cancer cell line, the half inhibitory concentration is 53 μg/mL. This result is highly promising, indicating that vanadium

Table 3. Statistical values of SW480 colon cancer cell line of VO_2 NPs.

Concentration mg/ml	Relative Cell Viability %	Number of Values	Standard deviation
7.81	97.06	8	0.027
15.625	80.43	8	0.024
31.25	47.28	8	0.026
62.5	44.42	8	0.028
125	21.67	8	0.025
250	19.46	8	0.025
500	13.83	8	0.021

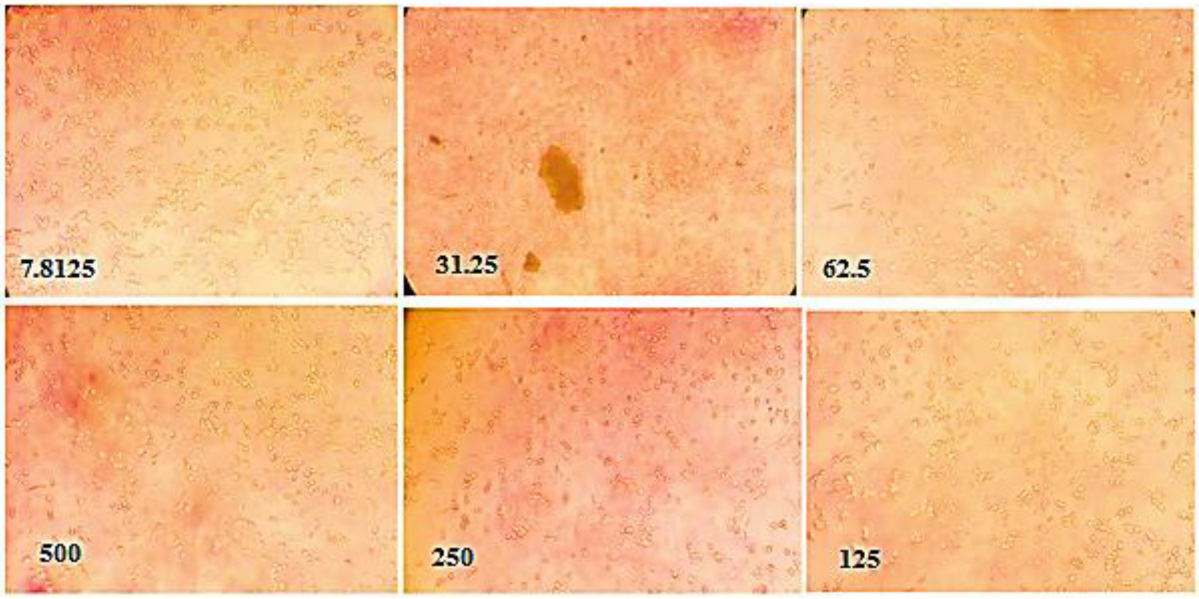

Fig. 10. Cancer cells treated with VO_2 NPs at different concentrations in (mg/ml).

nanoparticles prepared from *Vitex agnus castus* extract can kill colon cancer cells. This outcome is significant in the use of selective treatment for colon cancer, as illustrated in Figs. 9 and 10.

Conclusion

Vanadium oxide nanoparticles were synthesized using a green approach employing *Vitex agnus castus* extract and vanadium sulfate $VOSO_4.H_2O$. The resulting crystals showed a mono-crystalline morphology with a diameter of 16.66 nm. The particles exhibited variable activity levels against four different bacterial strains, comprising two gram-positive (*Staph. aureus, S. pneumonia*) and two gram-negative strains (*P. mirabilis, E.coli*). Furthermore, the particles demonstrated notable efficacy against *C.albicans*, a form of fungus, exhibiting the highest activity levels. In contrast, the toxicity of the nano-oxide was assessed on the SW480 colon cancer cell line, revealing an average inhibition of IC_{50} cells at 53 mg/ml. The findings of this study hold considerable importance in the use of selective treatment for colon cancer.

Acknowledgment

The author expresses sincere gratitude to the Chemistry Department, College of Education for Pure Sciences at Ibn-Al Haitham, University in Baghdad, Iraq, for providing resources for this research work.

Authors' declaration

- Conflicts of Interest: None.
- We hereby confirm that all the Figures and Tables in the manuscript are ours. Furthermore, any Figures and images, that are not ours, have been included with the necessary permission for republication, which is attached to the manuscript.
- Authors sign on ethical consideration's approval.
- Ethical Clearance: The project was approved by the local ethical committee at University of Baghdad.

The Authors' contribution statement

Both authors, S. H. M. and L. K. A. K., contributed equally in the conception and design of the study, data acquisition, analysis, interpretation, and drafting of the manuscript, as well as its subsequent revision and edits.

References

1. Salem SS, Hammad EN, Mohamed AA, El-Dougdoug W. A Comprehensive Review of Nanomaterials: Types, synthesis, characterization, and applications. Biointerface Res Appl Chem. 2023;13(1):1–30. https://doi.org/10.33263/BRIAC131.041.
2. Hameed HG, Abdulrahman NA. Preparation and characterization of TiO_2 nanoparticles with and without magnetic field effect via hydrothermal technique. Iraqi J Agric Sci. 2023;64(7):4125–4131. https://doi.org/10.24996/ijs.2023.64.7.3.
3. Farooqi ZUR, Qadeer A, Hussain MM, Zeeshan N, Ilic P. Characterization and physicochemical properties of nanomaterials. in nanomaterials: Synthesis, characterization, hazards and safety. Chap 5, MNT. 2021;97–121. https://doi.org/10.1016/C2020-0-00287-2.2.
4. Salem SS, Fouda A. Green synthesis of metallic nanoparticles and their prospective biotechnological applications. Biol Trace Elem Res. 2021;199:344–370. https://doi.org/10.1007/s12011-020-02138-3.
5. Jayasinghe ChD, Jayawardena UA, Dulashani RW, De Silva RM, Udagama PV. Honey mediated green synthesis of nanoparticles: New era of safe nanotechnology. J Nanomater. 2017;1–10. https://doi.org/10.1155/2017/5919836.
6. Hassan SS, Kadhim NJ, Jaber ZA. Synthesis, theoretical study, and biological evaluation of some metal ions with ligand "Methyl-6-[2-(4-Hydroxyphenyl)-2-((1-Phenylethylidene) Amino) Acetamido]-2,2-Dimethyl-5—Oxo-1-Thia-4-Azabicyclo [3.2.0] Heptane-3-Carboxyylate. Baghdad Sci J. 2023;20(1):0102. https://doi.org/10.21123/bsj.2022.6359.
7. Al-Bahadili ZR, AL-Hamdani AAS, Rashid FA, Al-Zubaidi LA, Ibrahim SM. An evaluation of the activity of prepared zinc nanoparticles with extracted alfalfa plant in the treatment of heavy metals. Baghdad Sci J. 2022;19(6):1399–1399. https://doi.org/10.21123/bsj.2022.
8. Bukhari A, Ijaz I, Gilani E, Nazir A, Zain H, Saeed R, *et al.* Green synthesis of metal and metal oxide nanoparticles using different plants' parts for antimicrobial activity and anticancer activity. Coat. 2021 Nov 9;11(11):1374. https://doi.org/10.3390/coatings11111374.
9. Qiu L, Zhu N, Feng Y, Michaelides EE, Żyła G, Jing D, *et al.* A review of recent advances in thermophysical properties at the nanoscale: From solid state to colloids. Phys Rep. 2020;843:1–81. https://doi.org/10.1016/j.physrep.2019.12.001.
10. Khan S, Mansoor S, Rafi Z, Kumari B, Shoaib A, Saeed M, *et al.* A review on nanotechnology: Properties, applications, and mechanistic insights of cellular uptake mechanisms. J Mol Liq. 2021;348(15):118008, https://doi.org/10.1016/j.molliq.2021.118008.
11. Alsahib SA, Baqer SR. Synthesis, identification of some new derivatives of 4-amino antipyrine bearing six and seven membered rings. J Phys Conf Ser. 2021;1853(1):012010. https://doi.org/10.1088/1742-6596/1853/1/012010.
12. Baqer SR, Alsammarraie A, Alias M, Al-Halbosiy M, Sadiq A. In vitro cytotoxicity study of Pt Nanoparticles decorated TiO_2 nanotube array. Baghdad Sci J. 2020;17:1169. https://doi.org/10.21123/bsj.2020.17.4.1169.
13. Ebrahimian J, Mohsennia M, Khayatkashani M. Photocatalytic-degradation of organic dye and removal of heavy metal ions using synthesized SnO_2 nanoparticles by vitexagnus-castus fruit via a green route. Mater Lett. 2020;263(15):127255. https://doi.org/10.1016/j.matlet.2019.127255.
14. Hamdouch A, Anejjar A, Bijla L, Gharby S, Asdadi A, Chebli B, *et al.* Corrosion inhibition of carbon steel by vitexagnuscastus leaves essential oils from the oasis of tata. Mor J Chem. 2023;11(1):105–118.https://doi.org/10.48317/IMIST.PRSM/morjchem-v11i1.37301.
15. Diniz MO, Golin AF, Santos MC, Bianchi RF, Guerra EM. Improving the performance of polymer-based ammonia gas sensor using POMA/V_2O_5 hybrid films. Org Electron. 2019 Apr 1;67:215–21. https://doi.org/10.1016/j.orgel.2019.01.039.
16. Dadkhah M, Tulliani JM. Green synthesis of metal oxides semiconductors for gas sensing applications. Sensors. 2022 Jun 21;22(13):4669. https://doi.org/10.3390/s22134669.
17. Gusain R, Gupta K, Joshi P, Khatri OP. Adsorptive removal and photocatalytic degradation of organic pollutants using metal oxides and their composites: A comprehensive review. J Adv Colloid Int Sci. 2019 Oct 1;272:102009. https://doi.org/10.1016/j.cis.2019.102009.
18. Ghani S, Rafiee B, Bahrami S, Mokhtari A, Aghamiri S, Yarian F. Comparison among the synthesis of some azomethine derivatives by classical and non-classical methods. Int J Drug Deliv Technol. 2021;11(2):515–517. https://doi.org/10.25258/ijddt.11.2.49.
19. Al Jabbar JL, Apriandanu DO, Yulizar Y, Sudirman S. Synthesis, characterization and catalytic activity of V2O5 nanoparticles using Foeniculumvulgare stem extract. IOP Conf. Ser: Mater Sci Eng. 2020 Feb 1;763(1):1–6 IOP Publishing. https://doi.org/10.1088/1757-899X/763/1/012031.
20. Hanooan WA, Qassim BB. A new green approach of CFIA technique for direct assay with a high throughput of sulfamethoxazole drugs using condensation reaction with NQS Agent. Baghdad Sci J. 2024;21(2):0369. https://doi.org/10.21123/bsj.2023.8104.
21. Almuslamawy HAJ, Aldhrub AHA, Ahmed SA, Mouhamad RS. Microbial simultaneous eradication from wastewater of sulphate and heavy metals. Asian J Water Environ Pollut. 2023;20(3):85–90. 10.3233/AJW230041.
22. Abdul Karem LK, Radhi IM, Mohammed SS. Biological activity of complexes of some amino acid: Review. Indian J Forensic Med Toxicol. 2020;14(4):2254–2261. https://doi.org/10.37506/ijfmt.v14i4.11888.
23. Shvets P, Dikaya O, Maksimova K, Goikhman A. A review of raman spectroscopy of vanadium oxides. Adv Colloid Interface Sc. 2019 Aug;50(8):1226–44. https://doi.org/10.1002/jrs.5616.
24. Ali A, Al-Hassani R, Hussain D, Jabir M, Meteab M. Antiproliferative activity and tubulin targeting of novel micro and nanoparticles complexes of 4-Amino-3-Thion-1,2,4-Triazole derivatives. Nano Biomed Eng. 2020;12(1):75–89. https://doi.org/10.5101/nbe.v12i1.p75-89.
25. Hassan SS, Ibrahim SK, Mahmoud MA, Alias MF. Synthesis and characterization of some metal complexes with new ligand ($C_{15}H_{10}N_4O_7SCl$) & theoretical treatment. Sys Rev Pharm. 2020;11(12):747–753. https://doi.org/10.31838/srp.2020.12.119.

26. Aliyu AO, Garba S, Bognet O. Green synthesis, characterization and antimicrobial activity of vanadium nanoparticles using leaf extract of moringaoleifera. Int J Chem Sci. 2018 Jan;11(1):42–48. https://doi.org/10.9790/5736-1101014248.
27. Kumar JA, Krithiga T, Maniganda S, Sathish S, Renita AA, Prakash P, *et al.* A focus to green synthesis of metal/metal based oxide nanoparticles: Various mechanisms and applications towards ecological approach. J Clean Prod. 2021;324(15):129198, https://doi.org/10.1016/j.jclepro.2021.129198.
28. Abeed BS, Al-Shmgani HS, Khalil KA, Mohammed HA. Evaluation of the potential protective role of galangin associated with gold nanoparticles in the histological and functional structure of kidneys of adult male albino mice Musmusculus administration with carbon tetrachloride. Ibn al-Haitham J Pure Appl. Sci. 2023;36(3):72–84.https://doi.org/10.30526/36.3.3250.
29. Rashid KW, Karem LKA, Rasheed MK. Synthesis, characterization and bioactivity study of few metal complexes of curcumin with 2-(1H-Benzimidazol-2-yl) aniline. Int J Drug Deliv Technol. 2022;12(3):1076–1080. https://doi.org/10.25258/ijddt.12.3.25.
30. Afify HH, Hassan SA, Obaida M, Abouelsayed A. Influence of annealing on the optical properties of monoclinic vanadium oxide VO2 prepared in nanoscale by hydrothermal technique. Phys E: Low-Dimens Syst. 2019;114:113610. https://doi.org/10.1016/j.physe.2019.113610.
31. Al-Saadi TM, Kamil ZA. Study the effect of manganese ion doping on the size-strain of SnO_2 nanoparticles using X-ray diffraction data. Ibn al-Haitham J Pure Appl Sci. 2023;36(3):158–166. https://doi.org/10.30526/36.3.3052.
32. Subramanian M, Dhayabaran VV, Shanmugavadivel M. Room temperature fiber optic gas sensor technology based on nanocrystalline Ba_3 (VO_4) $_2$: Design, spectral and surface science. Mater Res Bull. 2019 Nov 1;119:110560. https://doi.org/10.1016/j.materresbull.2019.110560.
33. Al-Saadi TM. Investigating the structural and magnetic properties of nickel oxide nanoparticles prepared by precipitation method. Ibn al-Haitham J Pure Appl Sci. 2022;35(4):94–103. https://doi.org/10.30526/35.4.2872.
34. Peng J, Guo J, Ma R, Jiang Y. Water-solid interfaces probed by high-resolution atomic force microscopy. Surf Sci Rep. 2021;77(1):100549. https://doi.org/10.1016/j.surfrep.2021.100549.
35. Nabhan KJ, Mahdi AS, Al-Zaidi BH, Ismail AH, Nasif ZN. New tetra-dentate schiff base ligand N_2O_2 and its complexes with some of metal ions: Preparation, identification, and studying their enzymatic and biological activities. Baghdad Sci J. 2022;19(1):0155. https://doi.org/10.21123/bsj.2022.19.1.0155.
36. Yousif M, Karem LKA. Synthesis, characterization and biological study of new complexes schiff base derived from 4-Bromo-2-Methylanine. Biochem Cell Arch. 2021;21:1941–1947.
37. Ahmed A, Majeed IY, Asaad N, Ahmed RM, Kamil GM, Abdul Rahman S. Some 3,4,5-trisubstituted-1,2,4-triazole synthesis, antimicrobial activity, and molecular docking studies. Egypt J Chem. 2022;65(3):395–401. https://doi.org/10.21608/EJCHEM.2021.93025.4397.
38. Abdulsada FM, Hussein NN, Sulaiman GM. Potentials of iron oxide nanoparticles (Fe_3O_4): As antioxidant and alternative therapeutic agent against common multidrug-resistant microbial species. Iraqi J Sci. 2023;64(6):2759–2773. https://doi.org/10.24996/ijs.2023.64.6.10.
39. Mohan B, Shaalan N. Synthesis, spectroscopic, and biological activity study for new complexes of some metal ions with schiff bases derived from 2-Hydroxy Naphthaldehyde with 2-amine benzhydrazide. Ibn al-Haitham J pure Appl sci. 2023;36(1):208–224.https://doi.org/10.30526/36.1.2978.
40. Al-Hadi Bahaa A, Othman Eman A, Karem LKA. Synthesis, characterization, and biological studies of new complexes derived from 2-(1H-benzimidazol-2-yl) aniline. Int J Drug Deliv Technol. 2021;11(3):937–941. https://doi.org/10.25258/ijddt.11.3.48.
41. Baqer SR, Alsammarraie AMA, Alias M, Al-Halbosiy MM, Sadiq AS. In vitro cytotoxicity study of Pt nanoparticles decorated TiO_2 nanotube array. Baghdad Sci J. 2020;17(4):1169–1169. https://doi.org/10.21123/bsj.2020.17.4.1169.
42. Mahmoud WH, Deghadi RG, Mohamed GG. Metal complexes of ferrocenyl-substituted schiff base: Preparation, characterization, molecular structure, molecular docking studies, and biological investigation. J Organo met Chem. 2020;917(20):121113.https://doi.org/10.1016/j.jorganchem.2020.121113.
43. Uddi MN, Ahmed SS, Alam SR. Biomedical applications of schiff base metal complexes. J Coord Chem. 2020;73(23):3109–3149.https://doi.org/10.1080/00958972.2020.1854745.
44. Abdalameer NK, A. Khaleefa T. Evaluation of antimicrobial activity using cadmium oxide nanoparticles prepared by physical method (PLAL). Ibn Al-Haitham J Pure Appl Sci. 2025;38(1):131–4. https://doi.org/10.30526/38.1.3716.
45. Abdel-Tawab M. Considerations to be taken when carrying out medicinal plant research—what we learn from an insight into the IC_{50} values, bioavailability and clinical efficacy of exemplary anti-inflammatory herbal components. Pharmaceuticals. 2021;14(5):437. https://doi.org/10.3390/ph14050437.

التحضيرالحيوي والتشخيص ودراسة الفعالية البايلوجية ومضاد السرطان لدقائق اوكسيد الفناديوم النانوية باستخدام مستخلص نبات كف مريم

صبا حربي مهدي، لقاء خالد عبد الكريم

قسم الكيمياء ، كلية التربية للعلوم الصرفة ابن الهيثم، جامعة بغداد، بغداد، العراق.

الخلاصة

تتضمن الدراسة استخدام طريقة التصنيع الحيوي لإنتاج جسيمات الفناديوم النانوية والتي تتميز بكونها رخيصة الثمن وسهلة الاستخدام و آمنة. تم تحضير دقائق اوكسيد الفناديوم النانوي من كبريتات الفناديوم الاحادي الماء $VOSO_4.H_2O$ مع مستخلص نباتي من عشبة كف مريم (Vitex agnus castus) وبتركيز (0.1 مولاري) من هيدروكسيد الصوديوم و تم إجراء التفاعل في وسط قلوي عند (8-12) pH والذي تميزت باستخدام العديد من التقنيات مثل ؛ مطياف الأشعة تحت الحمراءFT-IR ، مطيافية الأشعة فوق البنفسجية المرئية UV-Vis.، حيود الأشعة السينية XRD، المجهر الإلكتروني النافذ TEM، المجهر الالكتروني الماسح . SEM تم قياس الحجم البلوري للجسيمات النانوية باستخدام معادلة ديباي شيرر في حيود الأشعة السينية ، والذي كان 16.66 نانومتر،كذلك استخدام تقنية EDX والتي بينت نسبة عنصر الفناديوم ونسبة عنصر الاوكسجين مما يثبت تكون اوكسيد الفناديوم، بينما تم حساب حجم الجسيمات النانوية VO_2 باستخدام SEM وTEM. تم دراسة الأنشطة المضادة للميكروبات لجسيمات اوكسيد الفناديوم النانوي ضد اربع عزلات من البكتريا ، نوعان من *Staphylococcus aureus,* *Streptococcus pneumonia* تصبح موجبة لملون غرام ونوعان من *Proteus mirabilis*, *Escharia coli* سالبة لملون غرام ونوع واحد من الخميرة *Candida* حيث اظهر دقائق اوكسيد الفناديوم النانوية فعالية مختلفة ضد مضاد الميكروبات. كذلك، تم اختبار سمية الجسيمات النانوية المحضرة على خلايا الخط السرطاني SW480 لسرطان القولون وبتراكيز مختلفة باستخدام صبغة MTT، حيث وجد أن زيادة التركيز تؤدي إلى زيادة نسبة التثبيط، ومن حساب التثبيط النصفي للخلايا (IC50) والذي يساوي (53 mg/ml) يمكن القول أن هذا الاوكسيد النانوي يمكن استخدامه في العلاج الانتقائي لسرطان القولون.

الكلمات المفتاحية: الفعالية البايلوجية ، خط الخلية SW480، اوكسيدالنانوي, كف مريم ، حيود الاشعة السينية